Improved microwave SQUID multiplexer readout using a kinetic-inductance traveling-wave parametric amplifier

M. Malnou,[1,2,a)] J. A. B. Mates,[1] M. R. Vissers,[1] L. R. Vale,[1] D. R. Schmidt,[1] D. A. Bennett,[1] J. Gao,[1,2] and J. N. Ullom[1,2]
[1)] *National Institute of Standards and Technology, Boulder, Colorado 80305, USA*
[2)] *Department of Physics, University of Colorado, Boulder, Colorado 80309, USA*

(Dated: 3 May 2023)

We report on the use of a kinetic-inductance traveling-wave parametric amplifier (KITWPA) as the first amplifier in the readout chain of a microwave superconducting quantum interference device (SQUID) multiplexer (μmux). This μmux is designed to multiplex signals from arrays of low temperature detectors such as superconducting transition-edge sensor microcalorimeters. When modulated with a periodic flux-ramp to linearize the SQUID response, the flux noise improves, on average, from $1.6\,\mu\Phi_0/\sqrt{\mathrm{Hz}}$ with the KITWPA off, to $0.77\,\mu\Phi_0/\sqrt{\mathrm{Hz}}$ with the KITWPA on. When statically biasing the μmux to the maximally flux-sensitive point, the flux noise drops from $0.45\,\mu\Phi_0/\sqrt{\mathrm{Hz}}$ to $0.2\,\mu\Phi_0/\sqrt{\mathrm{Hz}}$. We validate this new readout scheme by coupling a transition-edge sensor microcalorimeter to the μmux and detecting background radiation. The combination of μmux and KITWPA provides a variety of new capabilities including improved detector sensitivity and more efficient bandwidth utilization.

Over the past few years, the multiplexed readout of transition-edge sensors (TES) with microwave superconducting quantum interference device (SQUID) multiplexers (μmux) has become ubiquitous. For example, this multiplexing technique will be deployed at the Simons Observatory to read out signals from tens of thousands of TES bolometers, aimed at measuring the cosmic microwave background[1]. It is also being used to read out TES microcalorimeter arrays for x-ray and gamma-ray spectroscopy[2–8].

A μmux divides the available readout bandwidth by coupling many readout resonators to a single transmission line. Each resonator is terminated by an rf-SQUID, inductively coupled to a TES, and this coupling is typically made large enough to ensure that the TES current noise dominates over the noise of the readout chain. For pulsed TES signals, this large inductive coupling results in a high flux slew rate at the SQUIDs, requiring a wide resonator bandwidth to track (see the supplementary material). In this context, having a lower readout noise would allow for a smaller coupling, a slower slew rate, narrower resonators, and therefore would allow us to increase the multiplexing factor.

Other sensors could benefit from a lower readout noise, in particular metallic magnetic calorimeters (MMCs). These devices place a magnetically susceptible calorimeter in the field of a superconducting loop that also passes through the input coil of a SQUID. With magnetic flux trapped in the loop, a variation in the MMC susceptibility shifts a fraction of this flux into or out of the SQUID. This shift of magnetic energy cannot be better resolved by increasing the inductive coupling to the SQUID. Furthermore, existing μmux readout techniques substantially degrade the performance of MMCs[9]. The use of a near-quantum-limited microwave amplifier could mitigate this problem and advance the use of multiplexed MMC arrays.

Traditionally, the first amplifier in the μmux readout chain is a high electron-mobility transistor (HEMT) amplifier, placed at 4 kelvin[2,3,10,11]. The HEMT offers several key features that make it compatible with μmux readout: (i) it provides sufficient gain, (ii) it is wideband, and (iii) it has a high compression power. However, its noise temperature, usually a few kelvin, is far from the lower bound imposed by quantum mechanics[12].

In this letter, we use a kinetic-inductance traveling-wave parametric amplifier[13–15] (KITWPA) as the first amplifier in the readout chain of a μmux. The KITWPA gain, bandwidth and power handling are also compatible with μmux readout, and its wideband noise has been shown to be close to the quantum limit[16,17]. It is placed before the HEMT, at millikelvin temperatures. With this readout scheme, we show that the flux noise attached to a coherent tone probing one of the resonators in the μmux, whose resonance is modulated at 3 MHz, is, on average, $0.77\,\mu\Phi_0/\sqrt{\mathrm{Hz}}$. When the KITWPA is turned off, the flux noise obtained with the HEMT as the first amplifier is more than doubled, reaching $1.6\,\mu\Phi_0/\sqrt{\mathrm{Hz}}$, a typical noise level for traditional μmux readout chains[11,18]. When the resonator is biased at its maximum flux-sensitive point, the open-loop flux noise drops from $0.45\,\mu\Phi_0/\sqrt{\mathrm{Hz}}$ (with the KITWPA off) to $0.2\,\mu\Phi_0/\sqrt{\mathrm{Hz}}$ (with the KITWPA on), equivalent to a system noise temperature of about 1 K. Such a low open-loop flux noise suggests that the demodulated flux noise could be decreased even further with straightforward improvements. Finally, we validate the use of the KITWPA coupled to the μmux by measuring pulse events in a TES microcalorimeter caused by background radiation.

Qualitatively, for microwave SQUID multiplexing, a low amplifier noise translates into a low flux noise. Each resonator within a μmux is terminated by an rf-SQUID,

[a)] Electronic mail: maxime.malnou@nist.gov

whose loop is coupled to a flux-bias line used to modulate the resonator's resonant frequency (see Fig. 1a). A probe tone, with frequency centered within the peak-to-peak frequency shift of the resonance, then describes a semi-circle trajectory in its rotating frame, at the modulation frequency. The readout noise attached to this tone can then be thought of as spreading its instantaneous position over a two-dimensional Gaussian in the rotating frame, along the in-phase (I) and out-of-phase (Q) quadratures (see Fig. 1b). It determines the noise on the tone's angle θ in this frame, and in turn, it determines the noise on the phase of θ (see Fig. 1c). This phase noise, multiplied by $\Phi_0/2\pi$, gives the flux noise.

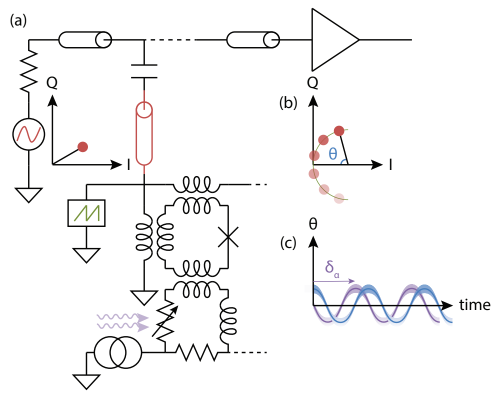

FIG. 1. Schematic of a µmux readout circuit, showing how amplifier noise translates to flux noise. In traditional µmux readout (a) a TES (shown as a variable resistor) is inductively coupled to a radio frequency (rf) SQUID embedded in a microwave resonator. (b) For a fixed microwave probe tone, the transmission moves along the resonance circle as a periodic function of flux in the SQUID. The noise associated with the amplifier chain (red disk) spreads the tone's position along the I and Q quadratures. (c) Under flux-ramp modulation, the SQUID is constantly sweeping out its approximately sinusoidal response. The noise attached to the tone thus translates into some noise on $\theta(t)$, the phase of the flux-ramp response. This noise impacts how well one can detect a phase shift δ_a on $\theta(t)$, due to a TES signal.

To reduce the flux noise, one can (i) increase the tone's power, but this power is eventually limited by the linearity of the SQUID response, and (ii) reduce the noise of the readout chain, which is what we propose to do, using a near-quantum-limited amplifier. In this context, for a given tone's power we can ask: what is the lowest flux noise achievable? In other words, what is the flux noise associated with a quantum-limited amplification chain?

Quantitatively now, starting with a system noise temperature T_{sys}, the (input-referred) noise power spectral density S_N along the I and Q quadratures of the tone is $S_N = k_B T_{\text{sys}}$, where k_B is the Boltzmann constant. Normalizing by the tone's power P_t, it translates into a spectral density on the rotation angle of the tone, θ, such that $S_\theta = 4k_B T_{\text{sys}}/P_t$[19]. Assuming a sinusoidal variation of θ with the flux Φ, $\theta(\Phi) = A\cos(2\pi\Phi/\Phi_0)$, with A the variation amplitude and Φ_0 the magnetic flux quantum, the maximum slope is then $\max\{d\theta/d\Phi\} = 2\pi A/\Phi_0$. At this maximum flux-sensitive point, the noise power spectral density on the flux is $\tilde{S}_\Phi = S_\theta \Phi_0^2/(2\pi A)^2$. Therefore, the flux noise $\sqrt{\tilde{S}_\Phi}$ at the maximum flux-sensitive point, sometimes called the *open-loop* flux noise, is:

$$\sqrt{\tilde{S}_\Phi} = \frac{1}{\pi A}\sqrt{\frac{k_B T_{\text{sys}}}{P_t}}. \tag{1}$$

For typical µmux operation, $A \simeq 1$; thus, with a system noise temperature $T_{\text{sys}} = 4\,\text{K}$, representative of a HEMT, and a probe tone power $P_t = -75\,\text{dBm}$, we obtain $\sqrt{\tilde{S}_\Phi} = 0.42\,\mu\Phi_0/\sqrt{\text{Hz}}$. Note that the dependence of the flux noise on the system noise temperature enters as a square root (due to the conversion from a power noise to an amplitude noise), so in practice, significantly reducing the flux noise is a difficult task. Note also that Eq. 1 gives the most honest way to quote T_{sys} knowing $\sqrt{\tilde{S}_\Phi}$, because here the system noise temperature includes all the possible sources of noise that contribute to the flux noise.

At the standard quantum limit (SQL), the noise power spectral density is equal to one photon[12], $S_N = \hbar\omega$, where $\hbar$ is the reduced Planck constant and ω is the angular frequency of the photon. Thus, at the SQL, $\sqrt{\tilde{S}_\Phi^{\text{SQL}}} = 1/(A\pi)\sqrt{\hbar\omega/P_t}$. For $\omega = 2\pi \times 4.5\,\text{GHz}$ and with $P_t = -75\,\text{dBm}$ (and $A = 1$) it means that $\sqrt{\tilde{S}_\Phi^{\text{SQL}}} = 0.1\,\mu\Phi_0/\sqrt{\text{Hz}}$. This is the quantum limit on the flux noise at the maximum flux-sensitive point, for this photon frequency and probe tone power.

In practice, the SQUIDs within the µmux are always modulated with a fast ramp of current[20], transforming the detector signal into a phase shift of the SQUID modulated flux response. This technique evades multiple sources of low-frequency noise. In this context, the flux noise $\sqrt{S_\Phi}$ on the demodulated tone is obtained from the open-loop flux noise, degraded twice: (i) when the peak-to-peak frequency shift of the resonator δ_f is comparable to its bandwidth B and when the modulation of θ is sinusoidal, the flux power spectral density integrated over the full 2π modulation of θ increases[20] by a factor of ≈ 2. (ii) Usually, the beginning of each ramp of current has a transient, which affects the modulation of θ. The transient is eliminated by discarding the first Φ_0 of the ramp response. Thus, if the ramp is swept over $n\Phi_0$, the noise increases by a factor $1/\alpha = n/(n-1)$. The general expression of the tone's *demodulated* flux noise is thus:

$$\sqrt{S_\Phi} = \frac{\sqrt{2/\alpha}}{\pi A}\sqrt{\frac{k_B T_{\text{sys}}}{P_t}}. \tag{2}$$

For example, with $A = 1$, $\alpha = 2/3$, $P_t = -75\,\text{dBm}$, and at the SQL where $k_B T_{\text{sys}} = \hbar\omega$, with $\omega = 2\pi \times 4.5\,\text{GHz}$, we would predict $\sqrt{S_\Phi^{\rm SQL}} = 0.17\,\mu\Phi_0/\sqrt{\rm Hz}$.

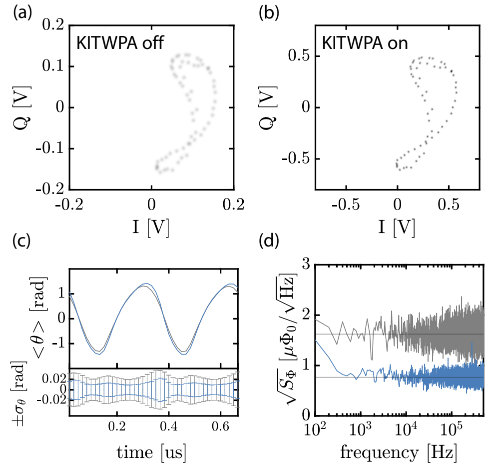

FIG. 2. Readout of a single resonator within the µmux, disconnected from a TES. The digitized output (at 60 MS/s) of the demodulated probe tone is obtained when the KITWPA is (a) off and (b) on; the origin of the I and Q quadrature frame is translated to the center of the circle supporting the tone's positions. The flux ramp sweeps $3\Phi_0$, at a frequency $f_r = 1\,$MHz (for 60 samples per ramp, 20 samples per Φ_0). The tone's power is $P_t \simeq -75\,$dBm, and the tone's frequency is $f_t = 4.383\,$GHz, to be compared to the resonator's maximal resonance $f_0 = 4.392\,$GHz and peak-to-peak frequency shift $\delta_f = 15\,$MHz. (c) For each sample within the ramp (excluding the 20 first samples corresponding to the first Φ_0) we measure a mean value and standard deviation for θ, the angle of rotation of the tone in the I and Q quadrature frame, when the KITWPA is off (gray line) and on (blue line). (d) Extracting a value for the phase of θ for each ramp segment, we Fourier transform this phase vector (and divide by 2π) to obtain the flux noise for the two situations: KITWPA off (gray line) and KITWPA on (blue line).

Microwave loss and excess noise will prevent the flux noise from reaching the SQL, so to see how much we can improve the flux noise in practice, we perform the readout of a µmux, using a KITWPA as our first amplifier, placed at millikelvin temperatures. Figure 2 shows the results of a single resonator readout within the µmux, for two situations: when the KITWPA is turned off (the HEMT is then the first amplifier in the chain), and when the KITWPA is turned on. This resonator is not connected to any TES, because otherwise the TES noise would overwhelm the readout noise (due to the engineered SQUID inductive coupling to the TES). We send a probe tone and apply a 1 MHz flux ramp to the SQUID, sweeping $3\Phi_0$ per ramp so that the resonance is modulated at $f_m = 3\,$MHz. Figure 2a (Fig. 2b) shows a histogram of the digitized output of the tone in its I and Q quadrature frame, obtained using a homodyne setup (see the supplementary material), when the KITWPA is off (on). The tone frequency and power are adjusted in this frame: at the optimal tone frequency the transmission describes a "figure-8" shape, due to the fact that the resonator is constantly driven out of equilibrium, and above the optimal probe tone power, $P_t \simeq -75\,$dBm, the resonator bifurcates. Qualitatively, when the KITWPA is turned on, the successive positions taken by the probe tone along the flux ramp are better defined, indicative of a lower phase noise. Quantitatively, Figure 2c shows $\langle\theta\rangle$ and σ_θ, respectively the mean value and standard deviation of θ over one ramp period (discarding the transient-contaminated first Φ_0) when the KITWPA is off and on. Clearly, turning on the KITWPA reduces σ_θ. It translates into a lower flux noise (see the supplementary material), $\sqrt{S_\Phi}$ (Fig. 2d), which drops from $1.6\,\mu\Phi_0/\sqrt{\rm Hz}$ to $0.77\,\mu\Phi_0/\sqrt{\rm Hz}$ on average.

Here, we compare the flux noise obtained when the KITWPA is off to when it is on, but the KITWPA-off situation is not equivalent to a standard µmux readout chain, with the HEMT as the first amplifier, because our chain contains extra microwave components. These components insert loss, and therefore increase the flux noise (see the supplementary material). Nonetheless, even with these components the flux noise with the KITWPA off remains low compared to standard values[11,18]. Furthermore, we used off-the-shelf microwave components to build the readout chain. These could be made more efficient, for example by integrating them on-chip, together with the KITWPA.

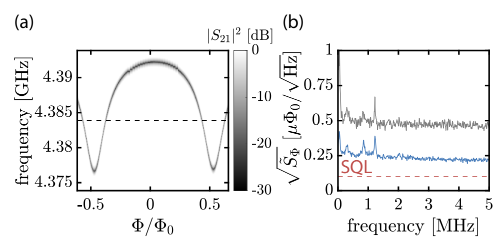

FIG. 3. Open-loop flux noise measurement. (a) The flux modulation curve of the resonator shows that $\delta_f = 15\,$MHz, while the bandwidth of the resonator is $B = 4.6\,$MHz. We set the tone's frequency f_t at $\max\{d\theta/d\Phi\}$ (dashed line), where $f_t = 4.384\,$GHz. (b) We measure the flux noise at this particular flux bias point (see the supplementary material), when the KITWPA is off (gray line) and on (blue line). In comparison, the flux noise of an amplification chain operating at the SQL is indicated by the dashed red line.

How close are we to the SQL? We cannot directly derive $T_{\rm sys}$ from Eq. 2, because in our case $\delta_f \gg B$, see Fig. 3a. It degrades $\sqrt{S_\Phi}$ compared to the situation where $\delta_f = B$, because when sweeping the ramp the tone then spends more time away from resonance, in the flux-insensitive region. Instead, to estimate $T_{\rm sys}$, we measure the open-loop flux noise at $\max\{d\theta/d\Phi\}$ (see the supplementary material), for the two situations, KITWPA off and on, see Fig. 3b. At 3 MHz, equal to the modulation frequency f_m previously used, $\sqrt{\tilde{S}_\Phi}$ drops from $0.45\,\mu\Phi_0/\sqrt{\mathrm{Hz}}$ to $0.2\,\mu\Phi_0/\sqrt{\mathrm{Hz}}$. Indeed, the open-loop flux noise is degraded by more than $\sqrt{2/\alpha}$ (with $\alpha = 2/3$) to yield the demodulated flux noise previously obtained. Using Eq. 1, $\sqrt{\tilde{S}_\Phi}$ corresponds to a system noise temperature $T_{\mathrm{sys}} = 4.6\,\mathrm{K}$ and $T_{\mathrm{sys}} = 0.9\,\mathrm{K}$, respectively (taking $A = 1$, and $P_t = -75\,\mathrm{dBm}$). In comparison, at the SQL, $T_{\mathrm{sys}}^{\mathrm{SQL}} = 0.2\,\mathrm{K}$ (at 4.5 GHz), therefore with the KITWPA turned on we operate 4.5 times above the quantum limit, whereas with the KITWPA off we operate more than 20 times above the quantum limit.

Reaching such low values for $\sqrt{\tilde{S}_\Phi}$ suggests two ways $\sqrt{S_\Phi}$ could be further reduced: (i) a resonator for which $\delta_f = B$ should, in principle, yield $\sqrt{S_\Phi} = \sqrt{2/\alpha}\sqrt{\tilde{S}_\Phi}$, so with $\alpha = 2/3$, $\sqrt{S_\Phi}$ could be as low as $0.35\,\mu\Phi_0/\sqrt{\mathrm{Hz}}$ (with the KITWPA on). (ii) With a tone tracking technique, where the tone's frequency is also modulated to follow the resonance, having $\delta_f \gg B$ becomes beneficial; in principle, this technique allows for a lower demodulated flux noise than the one obtained with a fixed-frequency tone[21].

To demonstrate that this amplification chain can truly be used for sensor readout, we connected another μmux channel to a TES (see the supplementary material). When the TES detects a photon or a particle, it generates a pulse of current in the SQUID loop, which translates into a dephasing event on the probe tone's trajectory (see Fig. 1). Absent any radiation, the flux noise is dominated by the TES noise at frequencies below 10 kHz, see Fig. 4a, and therefore there is no difference between the two situations, KITWPA off and on. In fact, the coupling to the TES within this μmux has been engineered to overwhelm higher readout noises than those obtained when using the KITWPA. With a redesign of the μmux, where both the coupling and the resonator bandwidth could be reduced with no penalty on the readout sensitivity, one would truly benefit from the near-quantum-limited nature of the readout chain.

Continuously acquiring the tone's excursion in the quadrature frame over several hours, we record the events for which Φ/Φ_0 significantly deviates from zero. These events correspond to cosmic rays and other background radiation hitting the TES (see the supplementary material). In Fig. 4b, we have overlapped the 226 events where $\Phi/\Phi_0 \leq 2$, detected over 3.5 hours with the KITWPA on (events with $\Phi/\Phi_0 > 2$ are present but excluded from the plot because the TES begins to saturate). This experiment shows both the successful operation of a TES in combination with a μmux and a KITWPA, and an improvement in the flux noise of the readout chain by use of the KITWPA.

In conclusion, we have demonstrated an unprecedented microwave SQUID multiplexing readout sensitivity, using a near-quantum-limited KITWPA as our first amplifier.

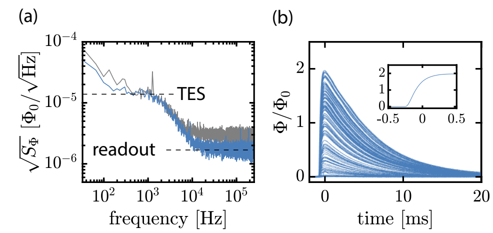

FIG. 4. Response of a resonator within the μmux, connected to a TES. (a) When the TES is biased between its normal and superconducting branches, the flux noise $\sqrt{S_\Phi}$ increases below 10 kHz, because the TES noise overwhelms the readout noise. At higher frequencies, we recover the improvement in flux noise when turning the KITWPA on (blue curve) compared to when the KITWPA is off (gray curve). Note that the flux noise values are higher here than in Fig. 2d, probably because of the unoptimized link (that includes long wire-bonds) between the TES and the μmux (see the supplementary material). (b) Pulse events due to background radiation have been detected by the TES over 3.5 hours. Focusing on times around 0 ms (inset) and on a single large amplitude pulse, it is evident that the KITWPA readout chain records the pulses without distortion even where the derivative of the flux signal is largest.

Modulating a μmux resonance at 3 MHz with a ramp, we showed that the flux noise of a demodulated tone is, on average, $\sqrt{S_\Phi} = 0.77\,\mu\Phi_0/\sqrt{\mathrm{Hz}}$, and it could be significantly lowered with straightforward improvements. In the context of μmux readout, the true system noise temperature must be calculated from the knowledge of the flux noise and the probe tone power. Here, our open-loop flux noise of $0.2\,\mu\Phi_0/\sqrt{\mathrm{Hz}}$ is equivalent to a system noise temperature of 0.9 K, or about 4.5 times above the quantum limit. Continuously monitoring over several hours the output of one resonator connected to a TES, we successfully measured the dynamic response of the sensor to background radiation, validating the use of this new amplification chain. This improvement of noise temperature should allow a doubling of μmux multiplexing factor for TES microcalorimeter readout, as well as enable the useful application of μmux to MMCs.

SUPPLEMENTARY MATERIAL

See the supplementary material for details on the bandwidth utilization with the flux ramp modulation, as well as details on the experimental setup, the flux noise measurement and processing, and on the KITWPA gain profile.

ACKNOWLEDGEMENTS

We thank D. T. Becker and D. S. Swetz for useful discussions. We gratefully acknowledge support from the NIST Program on Scalable Superconducting Computing, the National Aeronautics and Space Administration (NASA) under Grant No. NNH18ZDA001N-APRA, and the Department of Energy (DOE) Accelerator and Detector Research Program under Grant No. 89243020SSC000058.

[1] H. McCarrick, E. Healy, Z. Ahmed, K. Arnold, Z. Atkins, J. E. Austermann, T. Bhandarkar, J. A. Beall, S. M. Bruno, S. K. Choi, J. Connors, N. F. Cothard, K. D. Crowley, S. Dicker, B. Dober, C. J. Duell, S. M. Duff, D. Dutcher, J. C. Frisch, N. Galitzki, M. B. Gralla, J. E. Gudmundsson, S. W. Henderson, G. C. Hilton, S.-P. P. Ho, Z. B. Huber, J. Hubmayr, J. Iuliano, B. R. Johnson, A. M. Kofman, A. Kusaka, J. Lashner, A. T. Lee, Y. Li, M. J. Link, T. J. Lucas, M. Lungu, J. A. B. Mates, J. J. McMahon, M. D. Niemack, J. Orlowski-Scherer, J. Seibert, M. Silva-Feaver, S. M. Simon, S. Staggs, A. Suzuki, T. Terasaki, R. Thornton, J. N. Ullom, E. M. Vavagiakis, L. R. Vale, J. V. Lanen, M. R. Vissers, Y. Wang, E. J. Wollack, Z. Xu, E. Young, C. Yu, K. Zheng, and N. Zhu, "The simons observatory microwave squid multiplexing detector module design," The Astrophysical Journal **922**, 38 (2021).

[2] O. Noroozian, J. A. B. Mates, D. A. Bennett, J. A. Brevik, J. W. Fowler, J. Gao, G. C. Hilton, R. D. Horansky, K. D. Irwin, Z. Kang, D. R. Schmidt, L. R. Vale, and J. N. Ullom, "High-resolution gamma-ray spectroscopy with a microwave-multiplexed transition-edge sensor array," Applied Physics Letters **103**, 202602 (2013).

[3] J. A. B. Mates, D. T. Becker, D. A. Bennett, B. J. Dober, J. D. Gard, J. P. Hays-Wehle, J. W. Fowler, G. C. Hilton, C. D. Reintsema, D. R. Schmidt, D. S. Swetz, L. R. Vale, and J. N. Ullom, "Simultaneous readout of 128 x-ray and gamma-ray transition-edge microcalorimeters using microwave squid multiplexing," Applied Physics Letters **111**, 062601 (2017).

[4] W. Yoon, J. S. Adams, S. R. Bandler, D. Becker, D. A. Bennett, J. A. Chervenak, A. M. Datesman, M. E. Eckart, F. M. Finkbeiner, J. W. Fowler, J. D. Gard, G. C. Hilton, R. L. Kelley, C. A. Kilbourne, J. A. B. Mates, A. R. Miniussi, S. H. Moseley, O. Noroozian, F. S. Porter, C. D. Reintsema, J. E. Sadleir, K. Sakai, S. J. Smith, T. R. Stevenson, D. S. Swetz, J. N. Ullom, L. R. Vale, N. A. Wakeham, E. J. Wassell, and E. J. Wollack, "Toward large field-of-view high-resolution x-ray imaging spectrometers: Microwave multiplexed readout of 28 tes microcalorimeters," Journal of Low Temperature Physics **193**, 258–266 (2018).

[5] Y. Nakashima, F. Hirayama, S. Kohjiro, H. Yamamori, S. Nagasawa, A. Sato, S. Yamada, R. Hayakawa, N. Y. Yamasaki, K. Mitsuda, K. Nagayoshi, H. Akamatsu, L. Gottardi, E. Taralli, M. P. Bruijn, M. L. Ridder, J. R. Gao, and J. W. A. den Herder, "Low-noise microwave squid multiplexed readout of 38 x-ray transition-edge sensor microcalorimeters," Applied Physics Letters **117**, 122601 (2020).

[6] M. H. Carpenter, B. Stein, K. E. Koehler, C. J. Fontes, C. M. Smith, G. L. Wagner, Z. K. Baker, M. L. Handley, M. W. Rabin, P. Yang, E. R. Batista, D. G. McNeel, K. A. Schreiber, E. G. Bowes, J. N. Ullom, G. C. O'Neil, C. D. Reintsema, D. A. Bennett, G. C. Hilton, D. S. Swetz, D. R. Schmidt, J. A. B. Mates, D. T. Becker, J. C. Weber, J. D. Gard, K. M. Morgan, J. Imrek, D. Yan, A. L. Wessels, and M. Croce, "Hyperspectral x-ray imaging: Progress towards chemical analysis in the sem," IEEE Transactions on Applied Superconductivity **31**, 1–6 (2021).

[7] P. Szypryt, D. A. Bennett, W. J. Boone, A. L. Dagel, G. Dalton, W. B. Doriese, M. Durkin, J. W. Fowler, E. J. Garboczi, J. D. Gard, G. C. Hilton, J. Imrek, E. S. Jimenez, V. Y. Kotsubo, K. Larson, Z. H. Levine, J. A. B. Mates, D. McArthur, K. M. Morgan, N. Nakamura, G. C. O'Neil, N. J. Ortiz, C. G. Pappas, C. D. Reintsema, D. R. Schmidt, D. S. Swetz, K. R. Thompson, J. N. Ullom, C. Walker, J. C. Weber, A. L. Wessels, and J. W. Wheeler, "Design of a 3000-pixel transition-edge sensor x-ray spectrometer for microcircuit tomography," IEEE Transactions on Applied Superconductivity **31**, 1–5 (2021).

[8] P. Szypryt, N. Nakamura, D. T. Becker, D. A. Bennett, A. L. Dagel, W. B. Doriese, J. W. Fowler, J. D. Gard, J. Z. Harris, G. C. Hilton, *et al.*, "A tabletop x-ray tomography instrument for nanometer-scale imaging: demonstration of the 1,000-element transition-edge sensor subarray," arXiv preprint arXiv:2212.12073 (2022).

[9] M. Wegner, N. Karcher, O. Krömer, D. Richter, F. Ahrens, O. Sander, S. Kempf, M. Weber, and C. Enss, "Microwave squid multiplexing of metallic magnetic calorimeters: Status of multiplexer performance and room-temperature readout electronics development," Journal of Low Temperature Physics **193**, 462–475 (2018).

[10] B. Dober, D. T. Becker, D. A. Bennett, S. A. Bryan, S. M. Duff, J. D. Gard, J. P. Hays-Wehle, G. C. Hilton, J. Hubmayr, J. A. B. Mates, C. D. Reintsema, L. R. Vale, and J. N. Ullom, "Microwave squid multiplexer demonstration for cosmic microwave background imagers," Applied Physics Letters **111**, 243510 (2017).

[11] B. Dober, Z. Ahmed, K. Arnold, D. T. Becker, D. A. Bennett, J. A. Connors, A. Cukierman, J. M. D'Ewart, S. M. Duff, J. E. Dusatko, J. C. Frisch, J. D. Gard, S. W. Henderson, R. Herbst, G. C. Hilton, J. Hubmayr, Y. Li, J. A. B. Mates, H. McCarrick, C. D. Reintsema, M. Silva-Feaver, L. Ruckman, J. N. Ullom, L. R. Vale, D. D. Van Winkle, J. Vasquez, Y. Wang, E. Young, C. Yu, and K. Zheng, "A microwave squid multiplexer optimized for bolometric applications," Applied Physics Letters **118**, 062601 (2021).

[12] C. M. Caves, "Quantum limits on noise in linear amplifiers," Phys. Rev. D **26**, 1817–1839 (1982).

[13] B. H. Eom, P. K. Day, H. G. LeDuc, and J. Zmuidzinas, "A wide-band, low-noise superconducting amplifier with high dynamic range," Nature Physics **8**, 623–627 (2012).

[14] N. Zobrist, B. H. Eom, P. Day, B. A. Mazin, S. R. Meeker, B. Bumble, H. G. LeDuc, G. Coiffard, P. Szypryt, N. Fruitwala, I. Lipartito, and C. Bockstiegel, "Wide-band parametric amplifier readout and resolution of optical microwave kinetic inductance detectors," Applied Physics Letters **115** (2019), 10.1063/1.5098469, 042601.

[15] C. Joshi, W. Chen, H. G. LeDuc, P. K. Day, and M. Mirhosseini, "Strong kinetic-inductance kerr nonlinearity with titanium nitride nanowires," Phys. Rev. Appl. **18**, 064088 (2022).

[16] M. Malnou, M. Vissers, J. Wheeler, J. Aumentado, J. Hubmayr, J. Ullom, and J. Gao, "Three-wave mixing kinetic inductance traveling-wave amplifier with near-quantum-limited noise performance," PRX Quantum **2**, 010302 (2021).

[17] M. Malnou, J. Aumentado, M. Vissers, J. Wheeler, J. Hubmayr, J. Ullom, and J. Gao, "Performance of a kinetic inductance traveling-wave parametric amplifier at 4 kelvin: Toward an alternative to semiconductor amplifiers," Phys. Rev. Applied **17**, 044009 (2022).

[18] D. A. Bennett, J. A. B. Mates, J. D. Gard, A. S. Hoover, M. W. Rabin, C. D. Reintsema, D. R. Schmidt, L. R. Vale, and J. N. Ullom, "Integration of tes microcalorimeters with microwave squid multiplexed readout," IEEE Transactions on Applied Superconductivity **25**, 1–5 (2015).

[19] In fact, $S_N = R^2 S_\theta$, and when normalizing by the tone's power, $R = 1/2$ is the radius of the semi-circle in Fig. 1b.

[20] J. A. B. Mates, K. D. Irwin, L. R. Vale, G. C. Hilton, J. Gao, and K. W. Lehnert, "Flux-ramp modulation for squid multiplexing," Journal of Low Temperature Physics **167**, 707–712 (2012).

[21] C. Yu, Z. Ahmed, J. C. Frisch, S. W. Henderson, M. Silva-Feaver, K. Arnold, D. Brown, J. Connors, A. J. Cukierman, J. M. D'Ewart, B. J. Dober, J. E. Dusatko, G. Haller, R. Herbst,

G. C. Hilton, J. Hubmayr, K. D. Irwin, C.-L. Kuo, J. A. B. Mates, L. Ruckman, J. Ullom, L. Vale, D. D. Van Winkle, J. Vasquez, and E. Young, "Slac microresonator rf (smurf) electronics: A tone-tracking readout system for superconducting microwave resonator arrays," Review of Scientific Instruments **94**, 014712 (2023)

PLEASE CITE THIS ARTICLE AS DOI: 10.1063/5.0149646

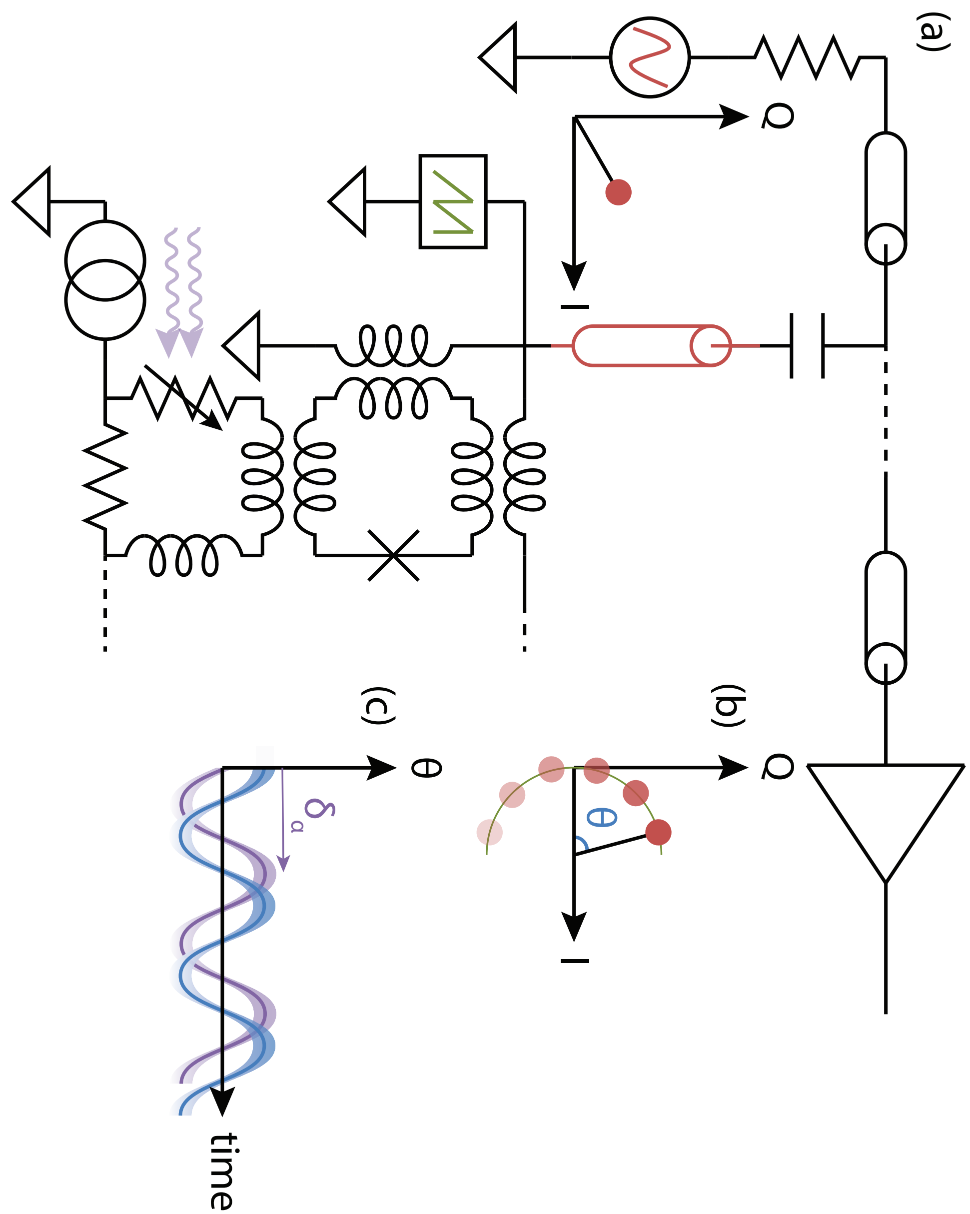

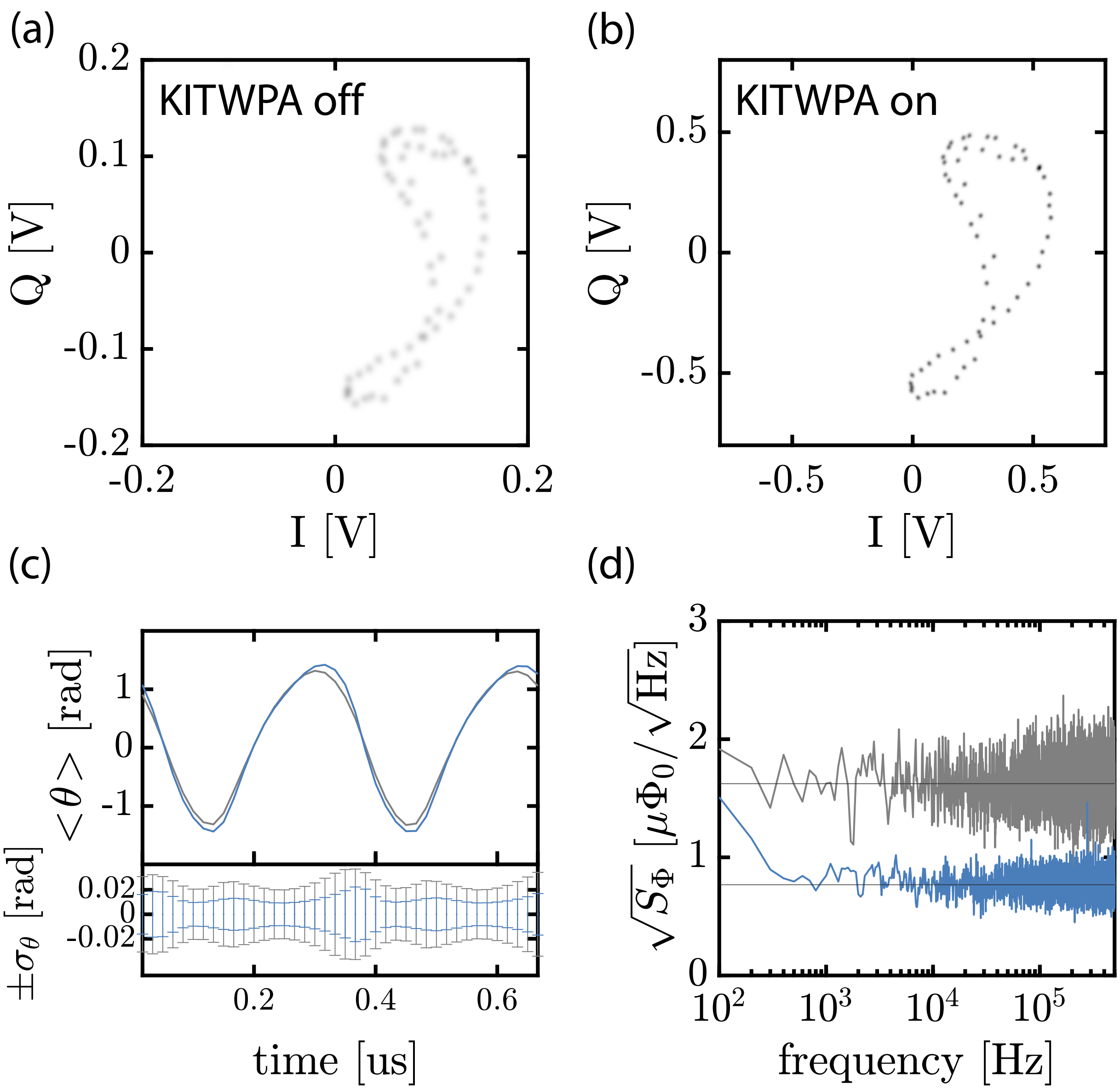
(a)
KITWPA off
Q [V]
I [V]
(b)
KITWPA on
Q [V]
I [V]
(c)
$<\theta>$ [rad]
$\pm\sigma_\theta$ [rad]
time [us]
(d)
$\sqrt{S_\Phi}$ [$\mu\Phi_0/\sqrt{\mathrm{Hz}}$]
frequency [Hz]

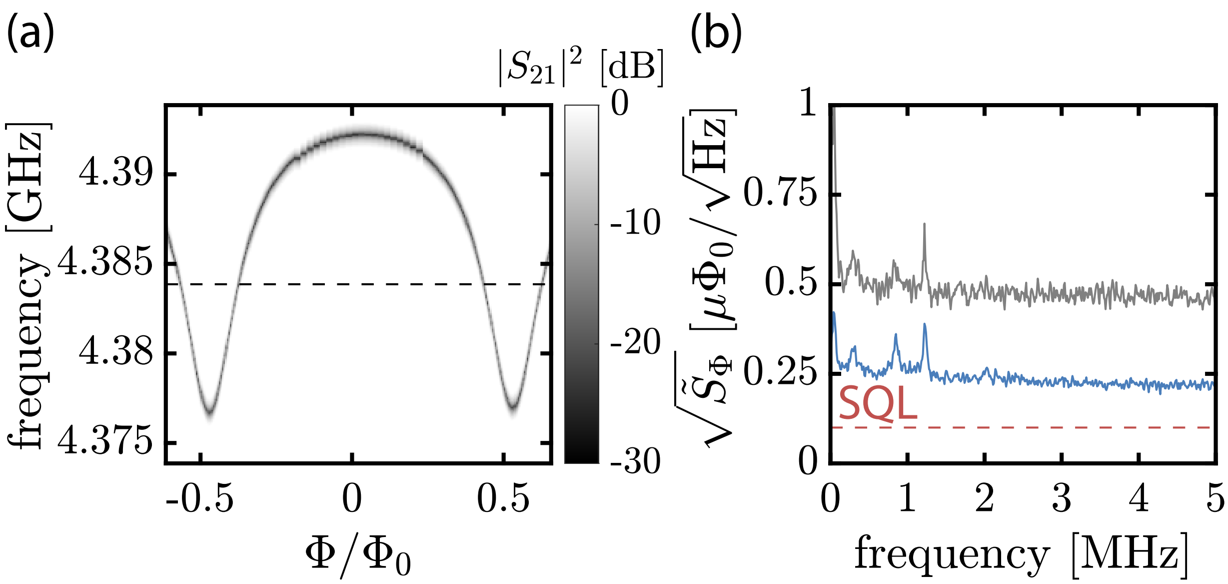
(a)
$|S_{21}|^2$ [dB]
0
-10
-20
-30
frequency [GHz]
4.39
4.385
4.38
4.375
-0.5
0
0.5
Φ/Φ_0
(b)
$\sqrt{\tilde{S}_\Phi}$ [$\mu\Phi_0/\sqrt{\mathrm{Hz}}$]
1
0.75
0.5
0.25
0
SQL
0
1
2
3
4
5
frequency [MHz]

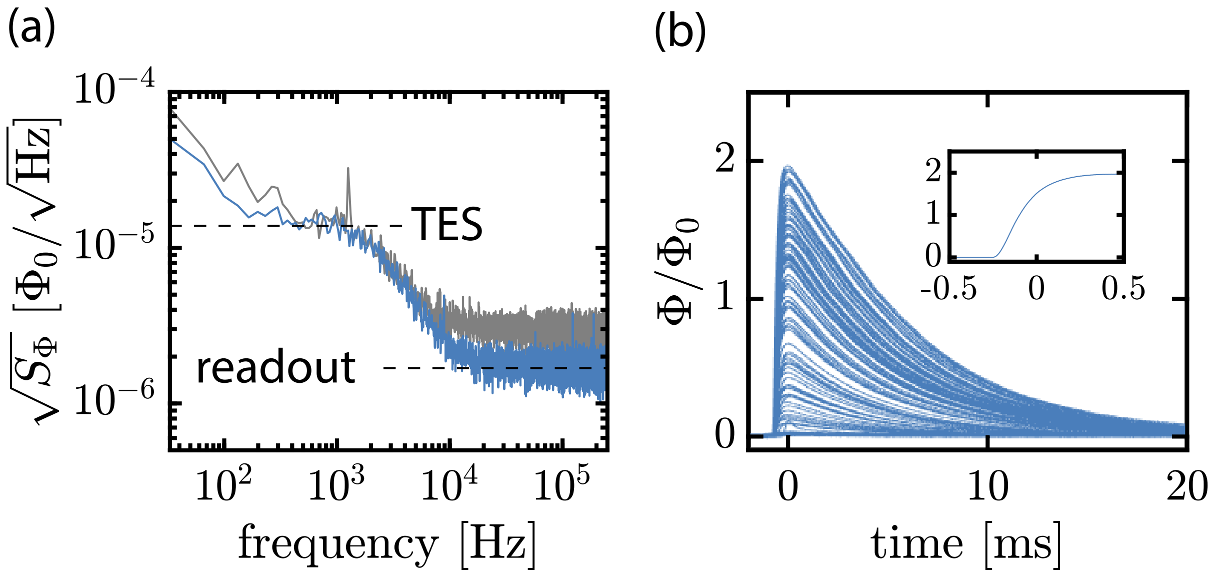
(a)
10^{-4}
10^{-5}
10^{-6}
TES
readout
$\sqrt{S_\Phi}$ $[\Phi_0/\sqrt{\mathrm{Hz}}]$
10^2
10^3
10^4
10^5
frequency [Hz]
(b)
Φ/Φ_0
0
1
2
-0.5
0.5
10
20
time [ms]